Journal of Mechanical Science and Technology, Vol. 19, No. 1, 〈Special Edition〉 pp. 343~349, 2005 343

Multibody Dynamics in Arterial System

Sang-Hoon Shin, Young-Bae Park
School of Oriental Medicine, Kyunghee University, Seoul 130-701, Korea
Hye-Whon Rhim
Biomedical Research Center, KIST, Hawolgok-dong, Seongbuk-gu, Seoul 136-791, Korea
Wan-Suk Yoo
Department of Mechanical Engineering, Pusan National University, Busan 609-735, Korea
Young-Jae Park
College of Oriental Medicine, Saemyung University, Jecheon, Chungbuk 390-711, Korea
Dae-Hun Park*
Cancer Experimental Resources Branch, National Cancel Center, Goyang, Gyeonggi 411-769, Korea

There are many things in common between hemodynamics in arterial systems and multibody dynamics in mechanical systems. Hemodynamics is concerned with the forces generated by the heart and the resulting motion of blood through the multi-branched vascular system. The conventional hemodynamics model has been intended to show the general behavior of the body arterial system with the frequency domain based linear model. The need for detailed models to analyze the local part like coronary arterial tree and cerebral arterial tree has been required recently. Non-linear analysis techniques are well-developed in multibody dynamics. In this paper, the studies of hemodynamics are summarized from the view of multibody dynamics. Computational algorithms of arterial tree analysis is derived, and proved by experiments on animals. The flow and pressure of each branch are calculated from the measured flow data at the ascending aorta. The simulated results of the carotid artery and the iliac artery show in good accordance with the measured results.

Key Words : Multibody Dynamics, Hemodynamics Arterial Tree System, Pulsatile Blood Flow, Vascular Impedance, Input Impedance, Arterial System Model, Forward & Backward Calculation

1. Introduction

Since William Harvey proved the circulation of blood in 1628, numerous attempts have been made to have a better insight into the circulatory system. Hemodynamics is a branch of fluid dynamics that deals with blood flow in the arterial system.

* Corresponding Author,
E-mail : dhj@ncc.re.kr
TEL : +82-31-920-2283; **FAX** : +82-31-920-0198
Cancer Experimental Resources Branch, National Cancel Center, Goyang, Gyeonggi 411-769, Korea. (Manuscript **Received** November 29, 2004; **Revised** December 15, 2004)

The repeated ejection of blood by the heart generates pressure and flow waves in the aorta, and the pulsatile flow is transformed into steady flow by the arterial tree. The classical view of the arterial system was the Windkessel model which characterized the entire arterial system as an elastic expansion chamber. This concept lasted until Young(1808) discuss the travel of waves in arteries. The first measurements of wave velocity were obtained by the Weber brothers in 1825. They attempted to relate wave velocity to the elastic properties of the vessel wall. This was later formulated by Moens and Korteweg in 1878.

The concept of vascular impedance plays an important part in discussion of the arterial sys-

tem. Until 1955, no reliable flow meter had been developed. So, flow information was obtained from pressure records. Womersley (1955a) made use of the concept of impedance in a study of pulsatile flows and pressure gradients. As soon as both flows and pressures could be measured, investigators tried to obtain input impedances. The first measurements of input impedances in the femoral artery of dogs were published by Randal (1956).

Womersley began with an analysis of flow in rigid tubes (Womersley, 1955a). He went on to develop a consistent treatment in elastic tubes (Womersley, 1955b) and eventually viscoelastic tubes (Womersley, 1957a). His results include the effects of external constraint by perivascular tissues (Womersley, 1957b) and the reflection of pulse waves (Womersley, 1958 ; Milnor, 1989).

For a detailed analysis of the dynamics of arterial blood flow, a model is required which includes the multi-branched configuration of the arterial system. Westerhoff (1969) developed an electrical model of human systemic arterial tree with 121 branches. Avolio (1976) developed a computer model based on the mathematical equations of the multi-branched model, where each segment is represented by sections of a linear non-uniform transmission line.

In this paper, computational algorithms of arterial tree analysis is derived, and proved by experiments on animals.

2. Materials and Methods

2.1 Computational algorithm of arterial tree analysis

2.1.1 Wave propagation in a tube

The wave propagation in the fluid-filled elastic tube is described (Duan, 1995) by,

$$\begin{aligned} &\frac{\partial q}{\partial t}+cZ_c\frac{\partial p}{\partial x}=0 \\ &\frac{\partial p}{\partial t}+\frac{c}{Z_c}\frac{\partial q}{\partial x}=0 \end{aligned} \tag{1}$$

where p and q are pressure and volumetric rate of flow in a tube respectively, and c is pulse wave velocity.

In Eq. (1), Z_C is characteristic impedance defined as,

$$Z_c=\frac{\rho c}{A} \tag{2}$$

where ρ is fluid density in a tube, and A is the cross sectional area of the tube.

Reflections are generated in a vascular system wherever there is a local change of impedance (Newman, 1983). Wave reflections in the tube have the effect of modifying the pressure and flow in the tube because the reflected waves combine with the forward traveling waves.

For the applied pressure $p_0e^{j\omega t}$ at the tube entrance, the solution of Eq. (1) is,

$$\begin{aligned} p(x,\ t)&=p_f(x,\ t)+p_b(x,\ t) \\ &=p_0e^{j\omega t-\gamma x}+\Gamma p_0e^{j\omega t+\gamma(x-2L)} \end{aligned} \tag{3}$$

where p_f is forward traveling pressure wave, p_b is backward traveling pressure wave, Γ is reflection constant (Zamir, 2000), and γ is wave propagation constant defined as

$$\gamma=j\frac{\omega}{c} \tag{4}$$

The solution for the flow of Eq. (1) is

$$\begin{aligned} q(x,\ t)&=q_f(x,\ t)+q_b(x,\ t) \\ &=Z_c(p_f(x,\ t)-p_b(x,\ t)) \end{aligned} \tag{5}$$

The concept of vascular impedance was borrowed from electrical engineering, and it is defined as

$$Z(x)=\frac{p(x,\ t)}{q(x,\ t)} \tag{6}$$

From Eqs. (3), (5), and (6), the input impedance of tube ($x=0$) is

$$Z_I=Z(0)=Z_c\frac{1+\Gamma e^{-2\gamma L}}{1-\Gamma e^{-2\gamma L}} \tag{7}$$

According to Eq. (6), if there is no wave reflection, the input impedance is the characteristic impedance.

The terminal impedance of tube ($x=L$) is

$$Z_T=Z(L)=Z_c\frac{1+\Gamma}{1-\Gamma} \tag{8}$$

The reflection constant Γ, determined from Eq. (8) is

$$\Gamma=\frac{Z_T-Z_C}{Z_T+Z_C} \tag{9}$$

The transmission ratio of pressure at the termination ($x=L$) to pressure at the origin ($x=0$) is

$$TP=\frac{p(L,\ t)}{p(0,\ t)}=\frac{1+\Gamma}{e^{\gamma L}+\Gamma e^{-\gamma L}} \tag{10}$$

2.1.2 Pulsatile blood flow in a vascular tube

The viscoelastic characteristics of vascular wall (Bergel, 1961) is represented as,

$$E_d=E_s e^{j\phi} \tag{11}$$

where E_s is the static value of Young's modulus of the vascular wall and ϕ represents the phase lead of pressure in relation to wall displacement.

The pulse wave velocity of inviscid fluid is defined by Moens-Korteweg equation (Milnor, 1989) as

$$c_0=\sqrt{\frac{E_s h}{2\rho R}} \tag{12}$$

Womersley (1955b) modeled the coupling effect of fluid and wall on the wave propagation as

$$c'=c_0\sqrt{\frac{1-F_{10}}{1-\sigma^2}} \tag{13}$$

where σ is Poisson ratio of arterial wall.

By considering of the viscoelastic property of vascular wall, the equation of wave velocity becomes

$$c=c' e^{j\frac{\phi}{2}} \tag{14}$$

From Eq. (3), the pressure and pressure gradient have the following relation with no reflection condition.

$$\frac{dp}{dx}=-\gamma\, p \tag{15}$$

The blood vessels are fully constrained by adjacent muscles and other tissues. With this constraint in mind, Womersley (1957b) suggested the following model

$$q=\frac{A\left(-\frac{\partial p}{\partial x}\right)}{j\omega\rho}(1-F_{10}) \tag{16}$$

where is function defined by Womersley (1957b).

From Eqs. (4), (14), (15), and (16), the characteristic impedance is

$$Z_C=\frac{\rho c_0}{A\sqrt{1-\sigma^2}}(1-F_{10})^{-\frac{1}{2}}\left(\cos\frac{\phi}{2}+j\sin\frac{\phi}{2}\right) \tag{17}$$

From Eqs. (4) and (14), the wave propagation coefficient is

$$\gamma=\frac{\omega}{c_0}\sqrt{\frac{1-\sigma^2}{1-F_{10}}}\left(\sin\frac{\phi}{2}+j\cos\frac{\phi}{2}\right) \tag{18}$$

2.1.3 Computational algorithm in arterial tree

Computational algorithm is summarized in Fig. 1. The configurations of arterial tree structure are defined, and then the characteristics of the vascular tube are inputted to the algorithm. The input impedances are calculated from peripheral arteries to ascending aorta, and then the flows and pressures are calculated from ascending aorta to peripheral arteries using the measured ascending aorta pattern.

Arterial trees are made up of large numbers of repeated bifurcations. A parent branch undergoes a furcation, then each of the child branches in turn furcated, and so on. The basic units of the tree structure are branch and node. A branch is composed of two nodes, which are input node and output node. The blood flow enters into the

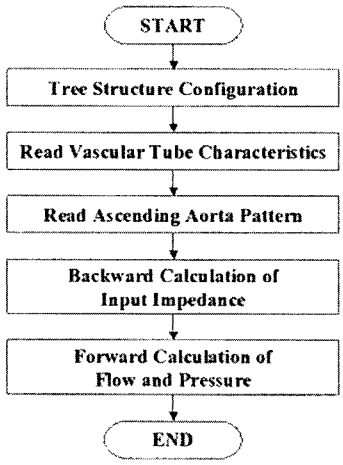

Fig. 1 Computational algorithm

input node, and comes out of the output node as shown in Figure 2.

The nodes and branches are numbered from ascending aorta to peripheral artery. Ascending aorta is the first branch and it called the initial branch. If there is no child branch, it is called 'terminal branch'.

Backward calculation of input impedance

Input impedance is calculated from the terminal branch (peripheral artery) to the initial branch (ascending aorta). Figure 3 shows the flowchart of the input impedance calculation. Input impedance is the function of the reflection constant, propagation constant, and characteristic impedance. The reflection constant is given in the case of the terminal branch, whereas calculated automatically with Eq. (9) in case of the other branches. Terminal impedance of the parent branch is the total input impedance of the child branches.

$$\frac{1}{(Z_T)_{parent}}=\sum\frac{1}{(Z_I)_{child}} \tag{19}$$

The characteristic impedance and the wave propagation coefficient is calculated by Eqs. (17) and (18), respectively.

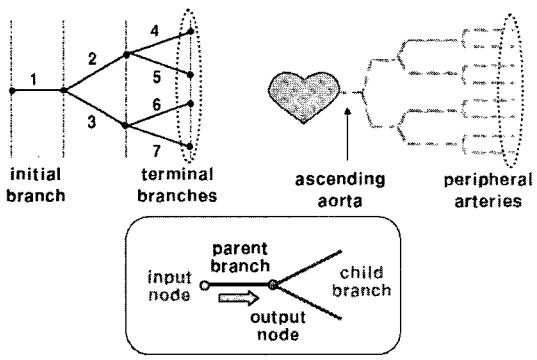

Fig. 2 Tree structure configuration

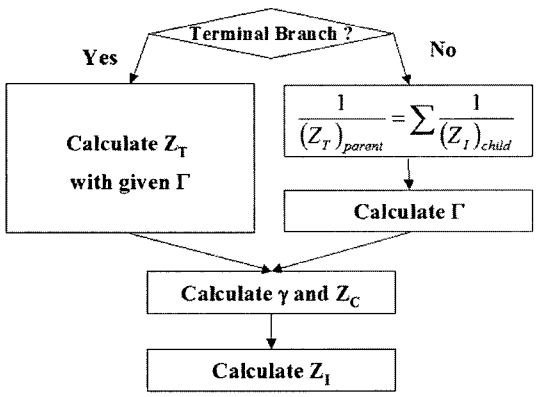

Fig. 3 Input impedance calculation

Forward Calculation of Pressure and Flow

Pressure and flow are calculated from ascending aorta (initial branch) to peripheral artery (terminal branch). To calculate the pressure and flow of every branch, pressure or flow pattern of ascending aorta must be known.

If the pressure pattern of the ascending aorta $p_1(t)$ is given, it is transformed into frequency domain data by Fourier Transformation,

$$P_1=F[p_1(t)] \tag{20}$$

where $F[\ ]$ is the Fourier Transformation operator.

Flow information in frequency domain is calculated by

$$Q_1=\frac{P_1}{(Z_I)_1} \tag{21}$$

Flow pattern in time domain is obtained from Inverse Fourier Transformation,

$$q_1(t)=F^{-1}[Q_1] \tag{22}$$

where $F^{-1}[\ ]$ is the inverse Fourier Transformation operator.

If the flow pattern of the ascending aorta $q_1(t)$ is given, the frequency domain data can be obtained by Fourier Transformation,

$$Q_1=F[q_1(t)] \tag{23}$$

Pressure information in frequency domain is obtained by

$$P_1=(Z_I)_1\cdot Q_1 \tag{24}$$

Pressure pattern in time domain is obtained from Inverse Fourier Transformation

$$p_1(t)=F^{-1}[P_1] \tag{25}$$

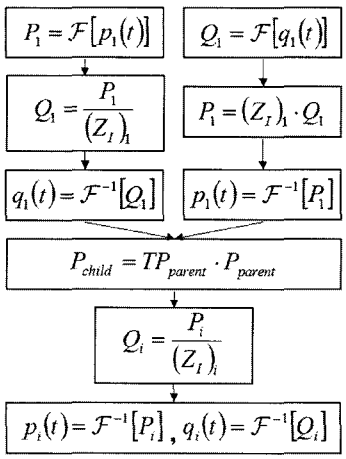

Fig. 4 Pressure and flow calculation

For the other branches, pressure can be calculated from the parent-child relation.

$$P_{child} = TP_{parent} \cdot P_{parent} \tag{26}$$

Flow information is calculated by

$$Q_i = \frac{P_i}{(Z_I)_i} \tag{27}$$

Pressure and flow in time domain are obtained from Inverse Fourier Transformation.

$$\begin{aligned} p_i(t) &= F^{-1}[P_i] \\ q_i(t) &= F^{-1}[Q_i] \end{aligned} \tag{28}$$

Computational algorithm is summarized in Figure 4.

2.2 Arterial model to rat

The arterial tree of a rat used in the experiment is shown in Figure 5. All rats were treated in strict accordance with the NIH Guide for the Humane Care and Use of Laboratory Animals. Animals were female Sprague-Dawley rats (Laboratory Animal Center in Seoul National University, Seoul, Korea). Before the experiments, they were maintained on a 12 : 12 H light : dark cycle and fed ad libitum.

The rats were anesthetized with ketamine HCl (150 mg/kg, i.p., Yuhan Ketamine 50 inj., Yuhan Co.), were perfused transcardially with saline in arteries and were fixed with 4% formalin solution. The diameters and lengths of arterials were

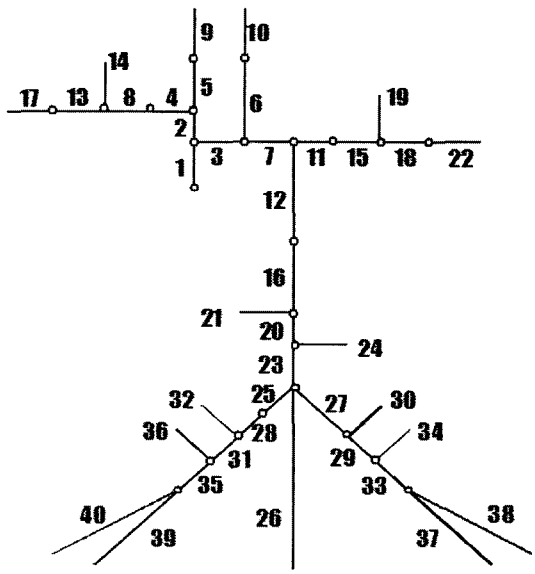

Fig. 5 Arterial tree of rat

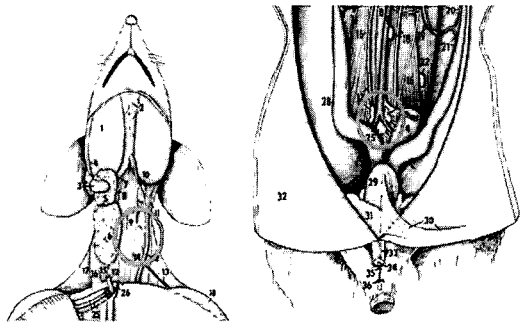

Fig. 6 Measuring point
(Left : Carotid A. Right : Iliac A.)

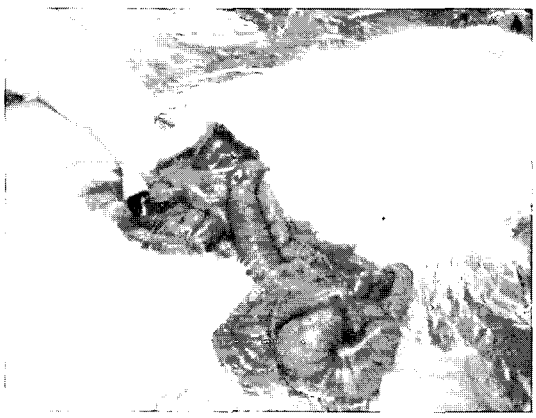

Fig. 7 Measurement at Iliac A

measured with a calibrator (Digimatic caliper, No. 500, Mitutoyo Cooperation). The measured data is shown in Table 1.

The weights of animals were about 320 g. They were anesthetized with enflurane (Gerolan soln., Choonhgwae Pharmacy Co.) with inhalation equipment (Multi-plus, Royal Medical Co. Ltd., Korea & TOPO Dual Mode Ventilator, Kent Scientific).

A non-invasive electromagnetic flow meter (Square-wave Electromagnetic Flow meter, Carolina Medical, Inc) was used to measure the blood flow at the check points; ascending aorta, carotid artery and iliac artery. The measuring points are shown in Figure 6, and Figure 7 shows the process to measure at iliac A. The blood flow signals were recoded with MP100 system (Biopac Systems, Inc.). Data was sampled with 1000 Hz using 10 Hz low pass filter option.

3. Results

The arterial tree of a rat traced from anatomical measurement is shown in Fig. 5. The whole tree was divided into 24 branches and 40 nodes.

With the anatomical data (Shin, 2004), the simulated results are compared with the measured ones to prove the validity of the arterial tree analysis algorithm. Using the measured flow pattern of ascending aorta (branch No. 1) as the input of simulation, the simulated results of the carotid artery (branch No. 9) and the iliac artery (branch No. 28) are compared with measured ones. Figure 8 shows the measured flow pattern of ascending aorta. The results of comparisons are in Figs. 9 and 10. In Figs. 9 and 10, the simulated data are scaled to fit the measured data.

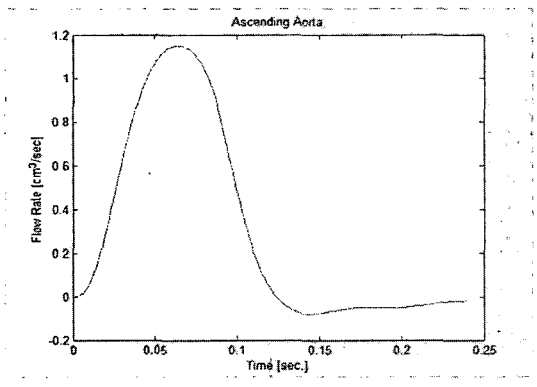

Fig. 8 Input flow pattern of ascending aorta

4. Discussion

We calculated the blood flow and pressure of each branch of the arterial tree with the input from the flow patterns measured at the ascending aorta. The simulated results are compared with the measured ones, which are measured at the carotid artery in the neck parts and the iliac artery in the abdominal parts.

The results of the carotid artery and the iliac artery for both the simulation and the measured ones are shown in Figs. 9 and 10. These results

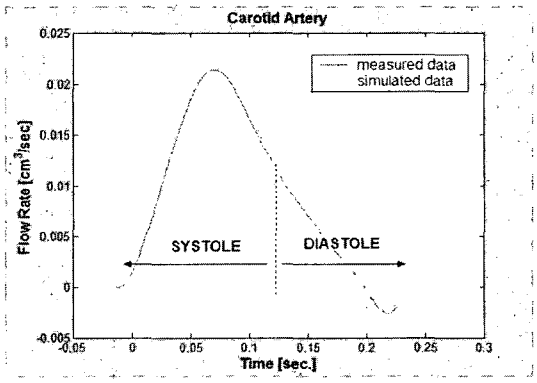

Fig. 9 Comparision of measurement and simulation (Carotid Artery)

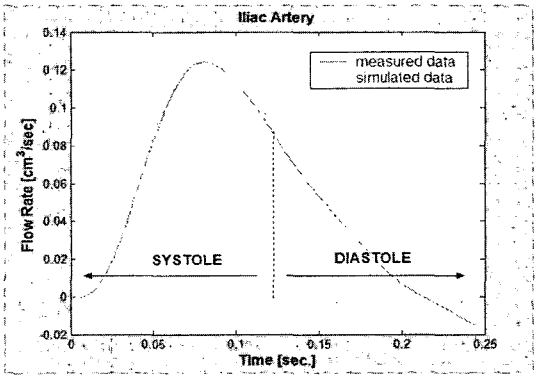

Fig. 10 Comparision of measurement and simulation (Iliac Artery)

show that during the systolic period both the simulation and the measurement have similar tendency. However, during the diastolic period this is not the case. Physiologically the close of aortic valve causes the rapid reduction of the blood flow. So, in the physiological point of view, the simulation shows more reasonable result than the measurement. The blood flow was measured by the non-invasive electromagnetic flow meter. The parts of the carotid artery (radius : 0.017 cm) and iliac artery (radius : 0.032 cm) have thin blood vessels with a small volume of blood. It seems that the measuring sensor that surrounded blood vessels generate the local curvature effect on a vascular tube. And this side effect makes the vascular tube work as one-way valve. Because of the complicated internal organs, the iliac artery in the abdominal parts showed more curvature effect than the carotid artery.

The anatomical structure of the human and the rat is very similar. The disorder of the blood circulation (pressure and flow) in the vascular system causes heart diseases and cerebrovascular disease, which have high death rates. The analysis of local areas such as the coronary artery in the heart and the cerebral artery in the brain has been increasingly required. In the future we can expect the detailed analysis of the multi-branched arterial system by applying the non-liner analysis techniques in the multibody dynamics to hemodynamics.

References

Avolio, A. P., 1980, "Multi-branched Model of the Human arterial System," *Medical & Biological Engineering & Computing*, Vol. 18, pp. 709~718.

Bergel, D. H., 1961, "The Dynamic Elastic Properties of the Arterial Wall," *Journal of Physiology*, Vol. 156, pp. 458~469.

Duan, B. and Zamir, M., 1995, Pressure Peaking in Pulsatile Flow Through Arterial Tree Structures," *Annals of Biomedical Engineering*, Vol. 23, pp. 794~803.

Milnor, W. R., 1989, *Hemodynamics 2nd ed.*, Baltimor, Williams & Wilkins.

Newman, D. L., Greenwald, S. E. and Moodie, T. B., 1983, "Reflection From Elastic Discontinuities," *Medical & Biological Engineering & Computing*, Vol. 21, pp. 697~701.

Randall, J. E. and Stacy, R. W., 1956, Mechanical Impedance of the Dog's Hind Leg to Pulsatile Blood Flow," *American Journal of Physiology*, Vol. 187, pp. 94~98.

Shin, S. H., Park, Y. B. et al., 2004, "Multibody Dynamics in Arterial System," *Seoul, The second Asian Conference on Multibody Dynamics*, pp. 298~305.

Westerhof, N., Bosman, F., De Vries, C. J. et al., 1969, "Analog studies of the human systemic arterial tree," *Journal of Biomechanics*, Vol. 2, pp. 121~143.

Womersley, J. R., 1955a, "Method for the Calculation of Velocity, Rate of Flow and Viscous Drag in Arteries when the Pressure Gradient is Known," *Journal of Physiology*, Vol. 127, pp. 553~563.

Womersley, J. R., 1955b, Oscillatory Motion of a Viscous Liquid in a Thin-walled Elastic Tube. I. The Linear Approximation for Long Waves., Philosophical Magazine, Vol. 46, pp. 199~221.

Womersley, J. R., 1957a, "The mathematical Analysis of the Arterial Circulation in a State of Oscillatory Motion," Wright Air Development Center, Technical Report TR 56-614.

Womersley, J. R., 1957b, "Oscillatory Flow in Arteries : The Constrained Elastic Tube as a Model of Arterial Flow and Pulse Transmission," *Physics in Medicine and Biology*, Vol. 2, pp. 178~187.

Womersley, J. R., 1958, "Oscillatory Flow in Arteries : The Reflection of the Pulse wave at Junctions and Rigid Inserts in the Arterial System," *Physics in Medicine and Biology*, Vol. 2, pp. 313~323.

Zamir, M., 2000, *The Physics of Pulsatile Flow*, New York, Springer-Verlag.